ELSEVIER

Bone 39 (2006) 106–116

BONE

www.elsevier.com/locate/bone

The mechanical phenotype of biglycan-deficient mice is bone- and gender-specific

Joseph M. Wallace [a], Rupak M. Rajachar [a], Xiao-Dong Chen [c], Songtao Shi [c], Matthew R. Allen [d], Susan A. Bloomfield [d], Clifford M. Les [e], Pamela G. Robey [c], Marian F. Young [c], David H. Kohn [a,b,*,1]

[a] *Department of Biomedical Engineering, The University of Michigan, Ann Arbor, MI 48109-2099, USA*
[b] *Department of Biologic and Materials Sciences, The University of Michigan, Ann Arbor, MI 48109-1078, USA*
[c] *Department of Health and Human Services, National Institutes of Health, National Institute of Dental and Craniofacial Research, Craniofacial and Skeletal Diseases Branch, Bethesda, MD 20892, USA*
[d] *Department of Health and Kinesiology, Texas A&M University, TX 77843, USA*
[e] *Henry Ford Hospital, Bone and Joint Center, Detroit, MI 48202, USA*

Received 30 August 2005; revised 29 November 2005; accepted 30 December 2005
Available online 9 March 2006

Abstract

Biglycan (bgn) is a small leucine-rich proteoglycan (SLRP) enriched in the extracellular matrix of skeletal tissues. While bgn is known to be involved in the growth and differentiation of osteoblast precursor cells and regulation of collagen fibril formation, it is unclear how these functions impact bone's geometric and mechanical properties, properties which are integral to the structural function of bone. Because the genetic control of bone structure and function is both local- and gender-specific and because there is evidence of gender-specific effects associated with genetic deficiencies, it was hypothesized that the engineered deletion of the gene encoding bgn would result in a cortical bone mechanical phenotype that was bone- and gender-specific. In 11-week-old C57BL6/129 mice, the cortical bone in the mid-diaphyses of the femora and tibiae of both genders was examined. Phenotypic changes in bgn-deficient mice relative to wild type controls were assayed by four-point bending tests to determine mechanical properties at the whole bone (structural) and tissue levels, as well as analyses of bone geometry and bone formation using histomorphometry. Of the bones examined, bgn deficiency most strongly affected the male tibiae, where enhanced cross-sectional geometric properties and bone mineral density were accompanied by decreased tissue-level yield strength and pre-yield structural deformation and energy dissipation. Because pre-yield properties alone were impacted, this implies that the gene deletion causes important alterations in mineral and/or the matrix/mineral ultrastructure and suggests a new understanding of the functional role of bgn in regulating bone mineralization in vivo.

Keywords: Transgenic; Mechanical properties; Mineralization; Histomorphometry; pQCT

Introduction

The bone extracellular matrix (ECM) is approximately one-third organic material by weight. This organic portion of bone is composed of type I collagen (roughly 90%) and a multitude of non-collagenous proteins [1]. Since one of bone's primary functions is to provide a mechanical support system for muscular activity, skeletal structure and function are heavily influenced by mechanical principles [2]. The strength and toughness of bone are derived from the organized mineralization of the ECM [3–7],

* Corresponding author. Department of Biologic and Materials Sciences, University of Michigan, 1011 N. University Ave., Ann Arbor, MI 48109-1078, USA. Fax: +1 734 647 2110.
E-mail addresses: jmwallac@umich.edu (J.M. Wallace), rupakr@u.washington.edu (R.M. Rajachar), xdchen@uams.edu (X.-D. Chen), sshi@dir.nidcr.nih.gov (S. Shi), matallen@iupui.edu (M.R. Allen), sbloom@tamu.edu (S.A. Bloomfield), les@bjc.hfh.edu (C.M. Les), probey@dir.nidcr.nih.gov (P.G. Robey), myoung@dir.nidcr.nih.gov (M.F. Young), dhkohn@umich.edu (D.H. Kohn).
[1] Part of the work was performed on sabbatical at the NIDCR.

8756-3282/$ - see front matter © 2006 Elsevier Inc. All rights reserved.
doi:10.1016/j.bone.2005.12.081

which is dependent on many factors including age [8,9], gender [10–13], genetic makeup [14–17], anatomic location [18–20] and mechanical milieu [21–23]. Over the past 20 years, particular attention has been paid to a group of molecules in the ECM called small leucine-rich proteoglycans (SLRPs) which, during the development and repair of bone, regulate ECM organization and mineralization by interacting with other matrix molecules [24–26] and growth factors [27–31] and directing their function. Specifically, in in vitro studies, SLRPs interact with the surface of collagen fibrils, regulating fibril formation, size and morphology [26,32], while also being implicated in mineralization [24,33].

Biglycan (bgn) is a SLRP that is enriched in the ECM of bone and other specialized connective tissues including cartilage, muscle and the keratinocyte layer of the skin [27,34–36]. Bgn is an X-linked gene that plays a role in the postnatal spatial patterning of bone [37] and appears to be directly involved in the growth and differentiation of osteoblast precursor cells [30]. While extensive work has been performed trying to uncover the structure of bgn and its role in bone formation and mineralization at the molecular level [32,34,35,38], the role of bgn in regulating higher levels of organization, such as geometric and mechanical properties of bone, is not well understood. Bgn-deficient mice displayed reduced skeletal growth, characterized by reduced trabecular bone volume in the femora by 3 months of age and reduced cortical thickness in the femora at 9 months [39]. Consistent with reduced bone volume at 3 months of age, bgn-deficient males show trends toward decreased failure load and yield energy in the femora compared with wild type males, and these trends become statistically significant at 6 months [39]. Beyond these limited studies, the mechanical and geometric effects of bgn deficiency on bone are unknown.

In vitro, bone marrow stromal cells from bgn-deficient male mice show increased apoptosis and decreased proliferation compared to cells from wild type mice, as well as lower colony forming efficiency in response to exogenous TGF-β [38]. In the femoral metaphyses of 3-month-old bgn-deficient males, osteoblast number is decreased, while osteoclast number is unchanged compared to wild type littermates [39]. Consistent with these cellular responses, trabecular mineral apposition rate and bone formation rate are decreased. The collective tissue and cellular-level data suggest that the bone phenotype may be due to a deficiency in matrix formation and/or mineralization. Contrary to the response in males, trabecular bone volume was unaffected while mineral apposition rate was increased in bgn-deficient female tibiae compared to wild type females, suggesting a gender-specific response to bgn deficiency [40].

From studies of inbred [14–17] and congenic [20,41] mouse strains and identification of quantitative trait loci (QTLs) responsible for bone geometric and mechanical properties [11,13,42,43], it is known that the genetic control of bone is both local (bone- and regional-specific) and gender-specific. Furthermore, there is evidence of gender-specific effects associated with genetic deficiencies [40,44,45]. It is therefore hypothesized that a genetic disruption, in this case an engineered deletion of the gene encoding biglycan, will result in a cortical bone mechanical phenotype, defined here by geometric, material and mechanical properties, that is bone- and gender-specific. Because of biglycan's role in regulating bone matrix structural organization, the bgn-deficient mechanical phenotype will be manifested by decreased tissue-level strength which will detrimentally impact structural mechanical integrity. This study characterizes the bgn-deficient mechanical phenotype in mice at 11 weeks of age in the cortical bone at the mid-diaphysis of the femora and tibiae of both genders. Phenotypic changes relative to wild type controls are assayed by four-point bending tests to determine mechanical properties at the whole bone (structural) and tissue levels, as well as analyses of bone geometry and bone formation using histomorphometry.

Materials and methods

Animals

All animal procedures were performed at the National Institute of Dental and Craniofacial Research (NIDCR) with NIDCR Institutional Animal Care and Use Committee approval (NIDCR animal approval protocol #NIDCR 001-151). Inbred lines of bgn-deficient and wild type mice were bred on a C57BL6/129 background. Bgn-deficient mice were originally generated by homologous recombination in embryonic stem cells [39]. Genotyping of the F1 generation of mice was performed via standard polymerase chain reaction (PCR) using DNA extracted from the tail of each mouse. PCR products were determined using agarose gel electrophoresis yielding bands of 212 (wild type allele) and 310 (disrupted allele) base pairs.

To determine proper sample sizes for detecting effects of genotype across bones and gender, power calculations were performed based on measured differences and standard deviations in mechanical and geometric properties due to Bgn deficiency [39] using a value of $\alpha = 0.05$ and a power $(1 - \beta)$ of 0.80 [46]. Twenty mice from each gender (2 genotypes, 10 mice per group) were housed in standard cages and given access to food, water and cage activity ad libitum. In order to assess bone formation during the last 3 weeks of the experiment (8–11 weeks of age), all mice were given a single intraperitoneal (IP) injection of tetracycline (20 mg per kg body weight) at day −20 before sacrifice and a single IP injection of calcein (15 mg per kg body weight) at day −6 before sacrifice. All mice were sacrificed at 11 weeks of age, at which time body weight was measured and both femora and tibiae were harvested, stripped of soft tissue and stored in either 70% ethanol at 4°C (for peripheral quantitative computed tomography (pQCT) and histology) or in a Ca^{2+}-buffered saline solution at −65°C (for mechanical testing) [47].

Mechanical testing

Left femora and tibiae were tested to failure in 4-point bending in displacement control using a custom-designed, solenoid-driven loading apparatus with a support span (L) of 6 mm and a loading span of 4 mm at a rate of 0.01 mm/s [48]. Before testing, the length of each femur was measured from the greater trochanter to the most distal portion of the femoral chondyles and the length of each tibia was measured from the most proximal portion of the tibial chondyles to the most distal portion of the medial malleolus using digital calipers accurate to 0.01 mm (Mitutoyo, Aurora, IL). Femora were tested in the anterior–posterior (AP) direction (posterior surface in compression) with the middle of the bone positioned halfway between the two supports. Tibiae were tested in the medial–lateral (ML) direction (lateral surface in compression). The tibiae were positioned such that the most distal portion of the junction of the tibia and fibula (TFJ) was aligned with the left-most support point. During each test, load and deflection were recorded, from which structural strength (force at yield and ultimate force), energy or work (measured as the area under the force vs. displacement curve to yield and to failure), stiffness (the slope of the linear portion of the force vs. displacement curve) and deformation (displacement to

yield, total displacement and post-yield displacement) were derived at the whole bone level.

During each test, the bone was closely monitored and the point of fracture initiation was noted. Because fractures often propagated at an angle across the bone (i.e. oblique fractures), the half of the fractured bone containing both the fracture initiation site and a full planar section of bone at that site was processed for histology, embedded and sectioned as described below (see Histomorphometry section). The jagged edge of the bone was trimmed off, and a 200-μm-thick planar section was used to determine geometric parameters (average cortical thickness from four quadrants, cortical area and AP and ML diameters) using a light microscope and digital analysis software (Nikon Eclipse TE 300, Image Pro-Plus v4.5, Matlab v5.3). The moment of inertia about the axis of bending was measured from each section using a Matlab script [49]. Together with the load and deflection data, the distance from the centroid to the surface of the bone in tension, c, and moment of inertia were used to derive estimated tissue-level mechanical properties from standard beam-bending equations for 4-point bending:

$$\text{Stress} = \sigma = \frac{Fac}{2*I}\ (\text{MPa}) \qquad \text{Strain} = \varepsilon = \frac{6cd}{a(3L-4a)}*10^6(\mu\varepsilon).$$

In these equations, F is the force, d is the displacement, a is the distance from the support to the inner loading point (1 mm), L is the span between the outer supports (6 mm) and I is moment of inertia. The modulus of elasticity was calculated as the slope of the linear portion of the stress vs. strain curve.

Peripheral quantitative computed tomography (pQCT)

Ex vivo scans of right femora and tibiae from the male mice were performed using an XCT Research-M device (Stratec Corp., Norland, Fort Atkinson, WI) [37]. Machine calibration was performed using a hydroxyapatite cone phantom.

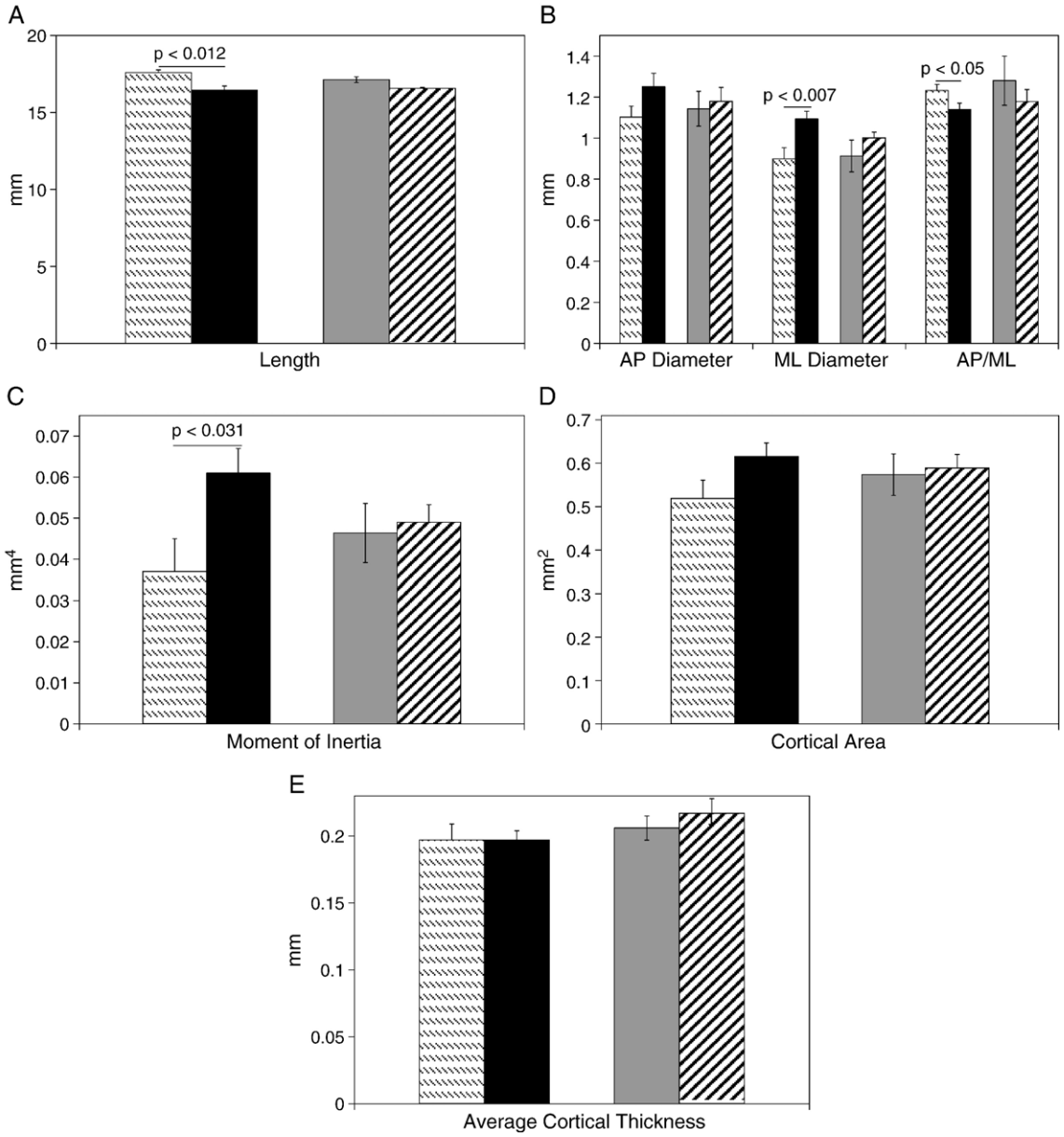

Fig. 1. Geometric properties of the male and female tibial diaphyses of biglycan-deficient vs. wild type mice. 11-week-old bgn-deficient males had decreased tibial length (A) with increased ML diameter (B) and moment of inertia (C) and an AP/ML closer to 1 versus wild type males. Cortical area (D) and cortical thickness (E) were unchanged compared with wild type males. No changes were noted in any properties in females. Data are presented as mean ± SEM. ▨ = wild type male, ■ = biglycan-deficient male, ▩ = wild type female, ▨ = biglycan-deficient female.

Table 1
Geometric properties of the male and female femoral diaphyses of biglycan-deficient vs. wild type mice

Group	Length (mm)	AP diameter (mm)	ML diameter (mm)	AP/ML	Moment of inertia (mm^4)	Average thickness (mm)
Male femora (wild type)	13.94 ± 0.82	1.16 ± 0.02	1.78 ± 0.12	0.67 ± 0.05	0.103 ± 0.003	0.224 ± 0.013
Male femora (bgn-deficient)	14.27 ± 0.25	1.18 ± 0.02	1.81 ± 0.03	0.65 ± 0.01	0.121 ± 0.007	0.237 ± 0.013
Female femora (wild type)	**14.42 ± 0.07**	1.23 ± 0.02	1.63 ± 0.04	**0.76 ± 0.03**	0.110 ± 0.007	0.224 ± 0.018
Female femora (bgn-deficient)	**13.67 ± 0.36**[b]	1.14 ± 0.05	1.76 ± 0.08	**0.65 ± 0.04**[b]	0.109 ± 0.013	0.247 ± 0.025

Data are presented as mean ± SEM. [b]Indicates $0.05 < P < 0.10$ vs. wild type for the same gender. Marginal differences are bolded for ease of interpretation.

Scans were performed at a CT speed of 2.5 mm/s with a voxel resolution of 0.07 × 0.07 × 0.50 mm and a scanning beam thickness of 0.50 mm. Two slices were scanned at the mid-diaphysis of each bone (50% of the total bone length ± 0.50 mm). A standardized analysis of diaphyseal bone (threshold of 700 mg/cm^3) was applied to each section. Values of total bone mineral content (BMC, coefficient of variation = ±1.18%) and total volumetric bone mineral density (vBMD, coefficient of variation = ±0.63%) obtained for each of the sites were averaged to get mean values.

Histomorphometry

Right tibiae from all animals (male bones were used following pQCT) were dehydrated in graded ethanol (70%, 95%, 100%) at 4°C, defatted in acetone and infiltrated in a liquid methyl methacrylate monomer (Koldmount™ Cold Mounting Liquid, Mager Scientific). The bones were then embedded in methyl methacrylate (Koldmount™ Cold Mounting Kit, Mager Scientific) and sectioned using a low-speed sectioning saw (South Bay Technology, Model 650, San Clemente, CA) with a diamond wafering blade (Mager Scientific, Dexter, MI). Sections 200 μm thick were made at the mid-diaphysis, 1 to 2 mm proximal to the TFJ, and were hand ground and polished to a final thickness of between 50 and 75 μm using wet silicon carbide abrasive discs. Sections were imaged using the Nikon DAPI-FITC-TRITC triple band filter combination (DAPI excitation at 385–400 nm and emission at 450–465 nm; FITC excitation at 475–490 nm and emission at 505–535 nm; TRITC excitation at 545–565 nm and emission at 580–620 nm) at a magnification of 200× and analyzed using digital analysis software (Nikon Eclipse TE 300, Image Pro-Plus v4.1). All histomorphometric analyses were performed using standard ASBMR methods and nomenclature [50]. Single- and double-labeled surfaces (sLs; dLs) were measured on both the endocortical and periosteal surfaces, from which endocortical and periosteal mineralizing surfaces (Es.MS; Ps.MS) were determined and normalized to the total corresponding surface length. The center-to-center interlabel distance was measured on each surface to determine mineral apposition rate (MAR). MS and MAR were further used to calculate bone formation rate (BFR = MAR * MS) at each surface.

Statistical analysis

All data are presented as mean ± standard error of the mean (SEM). Statistical analyses were performed on body mass and all geometric, mechanical, histomorphometric and bone mineral parameters in each gender and/or bone using an ANOVA checking for effects of genotype followed by post hoc Student–Newman–Keuls tests (Sigma Stat 2.0, Jandel Scientific). A value of $P < 0.05$ was considered significant, while a P value between 0.05 and 0.10 was also noted as a trend. In order to assess any predictive relationships between geometric and structural-level mechanical properties, tissue-level mechanical properties and structural-level mechanical properties or bone mineral density and structural or tissue-level mechanical properties, Pearson's Product–Moment Correlations were performed within each subgroup (e.g. bgn-deficient male tibiae).

Results

The geometric and mechanical phenotypes associated with bgn deficiency are bone- and gender-specific in 11-week-old mice. Bgn-deficient males exhibited geometric and mechanical changes almost exclusively in the tibiae (Figs. 1–4), with little effect seen in the femora (Tables 1–3). In contrast, bgn-deficient females demonstrated changes to a much lesser degree than the males and in the femora (Tables 1 and 2) rather than the tibiae (Fig. 2A). Both bgn-deficient males and females had significantly lower body mass at 11 weeks of age compared to wild types [(wild type male = 26.55 ± 0.61 g, bgn-deficient male = 23.73 ± 0.76 g; $P < 0.02$); (wild type female = 20.84 ± 0.60 g, bgn-deficient females = 17.56 ± 0.88 g; $P < 0.01$)].

Table 2
Structural mechanical properties of the male and female femoral diaphyses of biglycan-deficient vs. wild type mice

Group	Yield force (N)	Ultimate force (N)	Elastic deformation (mm)	Post-yield deformation (mm)	Total deformation (mm)	Stiffness (N/mm)	Work to yield (mJ)	Work to failure (mJ)
Male femora (wild type)	21.38 ± 2.68	29.06 ± 2.89	0.080 ± 0.15	0.061 ± 0.017	0.141 ± 0.024	274.3 ± 41.8	**1.06 ± 0.21**	2.63 ± 0.54
Male femora (bgn-deficient)	19.74 ± 2.19	30.21 ± 1.93	0.058 ± 0.01	0.060 ± 0.009	0.119 ± 0.010	314.3 ± 15.9	**0.62 ± 0.08**[a]	2.29 ± 0.27
Female femora (wild type)	26.01 ± 1.66	**35.91 ± 1.59**	0.066 ± 0.012	0.054 ± 0.008	**0.120 ± 0.014**	495.6 ± 38.0	1.02 ± 0.14	**2.75 ± 0.32**
Female femora (bgn-deficient)	24.86 ± 2.04	**30.94 ± 0.79**[a]	0.56 ± 0.008	0.032 ± 0.009	**0.088 ± 0.006**[b]	475.5 ± 66.9	0.90 ± 0.18	**1.83 ± 0.15**[a]

Data are presented as mean ± SEM. [a]Indicates $P < 0.05$ vs. wild type for the same gender, [b]indicates $0.05 < P < 0.10$ vs. wild type for the same gender. Significant and marginal differences are bolded for ease of interpretation.

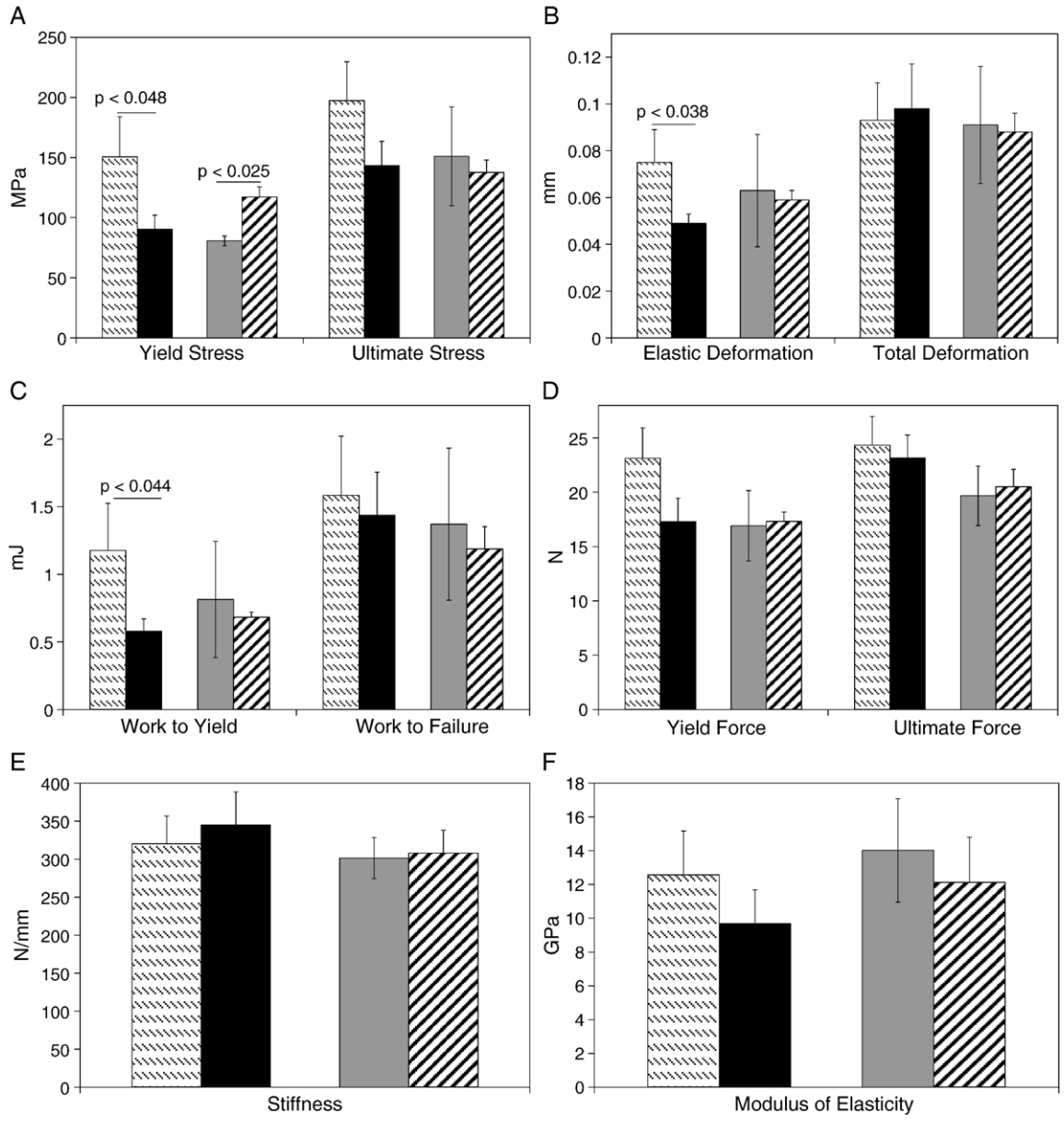

Fig. 2. Mechanical properties of the male and female tibial diaphyses of biglycan-deficient vs. wild type mice. 11-week-old bgn-deficient males displayed decreased tibial yield stress (A) and elastic deformation (B) as well as decreased work-to-yield (C) versus wild type males. Yield and ultimate forces (D), structural stiffness (E) and tissue modulus (F) were unchanged. In females, the only difference noted was an increase in yield stress (A) versus wild type females. Data are presented as mean ± SEM. ▨ = wild type male, ■ = biglycan-deficient male, ▩ = wild type female, ▨ = biglycan-deficient female.

Phenotypic changes in biglycan-deficient male tibiae

The most significant geometric and mechanical effects of bgn deficiency were displayed in the male tibiae (Figs. 1 and 2). Bgn-deficient male tibiae were significantly shorter than those of their wild type counterparts (Fig. 1A, $P < 0.012$). This decrease in longitudinal growth was in contrast to increased radial growth, characterized by increased ML width (Fig. 1B, $P < 0.007$) and moment of inertia (Fig. 1C, $P < 0.031$). Furthermore, the AP/ML ratio was significantly closer to a value of 1 in bgn-deficient males (Fig. 1B, $P < 0.05$). Improved geometric properties were not accompanied by changes in MS (Fig. 3A), MAR (Fig. 3B) or BFR (Fig. 3C), though endocortical surface trends suggest increased matrix formation activity in the bgn-deficient males (29%, 14% and 27% increases in Es.MS, Es.MAR and Es.BFR, respectively). The bgn-deficient male tibial diaphyses also had significantly greater vBMD (Fig. 4A, $P < 0.001$) than wild type males, though there was no change in BMC (Fig. 4B). Together with larger cross-sectional dimensions and increased mineral density, bgn-deficient male tibiae exhibited significant decreases in tissue-level yield strength (Fig. 2A, $P < 0.048$), structural elastic deformation (Fig. 2B, $P < 0.038$) and structural work-to-yield (Fig. 2C, $P < 0.044$), all of which are measures of pre-yield behavior. No statistically significant changes occurred in post-yield properties. There were significant negative correlations

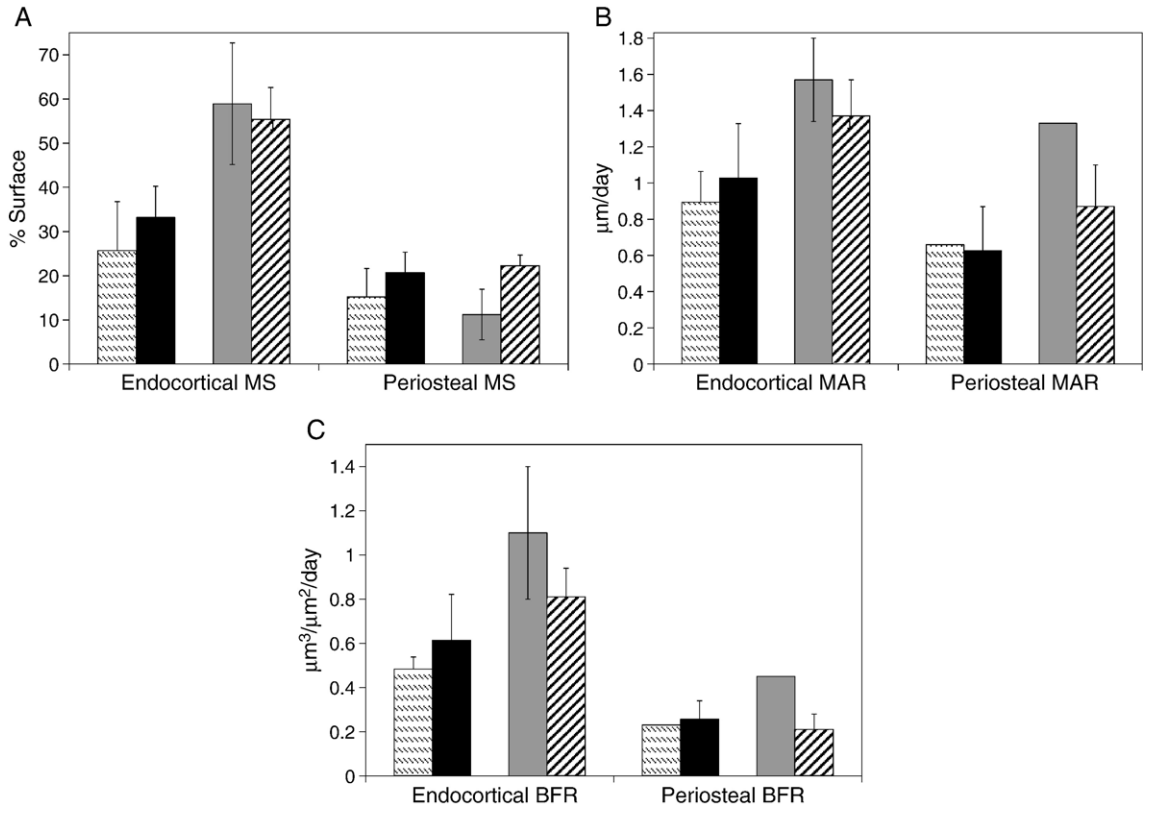

Fig. 3. Histomorphometry of the male and female tibial diaphyses of biglycan-deficient vs. wild type mice. Between 8 and 10 weeks of age, there were no significant differences in mineralizing surface (A), mineral apposition rate (B) or bone formation rate (C) in the male tibial diaphysis, though endocortical trends suggest increased activity in the bgn-deficient animals. Similarly, no differences were noted between wild type and biglycan-deficient females. Data are presented as mean ± SEM. ▨ = wild type male, ■ = biglycan-deficient male, ▩ = wild type female, ▨ = biglycan-deficient female.

between geometric properties (ML width and moment of inertia, independent variables) and tissue-level yield strength, structural elastic deformation and structural work-to-yield in the bgn-deficient mice (Fig. 5), but similar relationships did not exist in the wild type mice (data not shown). Furthermore, there was no correlation between vBMD and any geometric or mechanical properties in either genotype (data not shown).

Phenotypic changes in biglycan-deficient male femora

There were few differences in the geometric and mechanical properties of bgn-deficient male femora versus wild type males (Tables 1–3). There was a significant reduction in structural work-to-yield (Table 2, $P < 0.033$) and tissue-level yield strength (Table 3, $P < 0.026$) of the bgn-deficient male femoral diaphyses and a marginal increase in BMC (wild type: 1.06 ± 0.05 mg/mm, bgn-deficient: 1.29 ± 0.06 mg/mm; $P < 0.058$). Femoral length was not different between the two groups (Table 1), and no other geometric or material parameters were affected.

Phenotypic changes in biglycan-deficient female femora and tibiae

Bgn-deficient females expressed an altered mechanical phenotype to a lesser degree than the male mice and in the femur rather than the tibia (Figs. 1–3, Tables 1–3). There were significant decreases in femoral structural strength (Table 2, $P < 0.023$) and work-to-failure (Table 2, $P < 0.017$), and marginal decreases in femoral length (Table 1, $P < 0.075$), AP/ML ratio (Table 1, $P < 0.079$), total structural deformation (Table 2, $P < 0.067$) and tissue-level strain to failure ($P < 0.08$) in the bgn-deficient females. No other properties were affected in the femora. The bgn-deficient female tibiae displayed no differences in cross-sectional geometry relative to the wild types (Fig. 1). Tissue-level yield stress (Fig. 2A, $P < 0.025$) was significantly greater in bgn-deficient females. No other mechanical properties were different in the tibiae (Fig. 2), though periosteal mineralizing surface was marginally increased in bgn-deficient females compared to wild type animals (Fig. 3A, $P < 0.075$).

Discussion

The mechanical phenotype in bgn-deficient mice, characterized by geometric, material and mechanical properties, displayed bone and gender specificity in 11-week-old mice. In the two long bones examined in this study, bgn-deficient male mice exhibited geometric and mechanical changes almost exclusively in the tibial diaphysis with little effect in the femora. While several studies have shown bone-specific responses to stimuli like exercise [18,51] and hormonal treatment [19], most investigations evaluate multiple cancellous

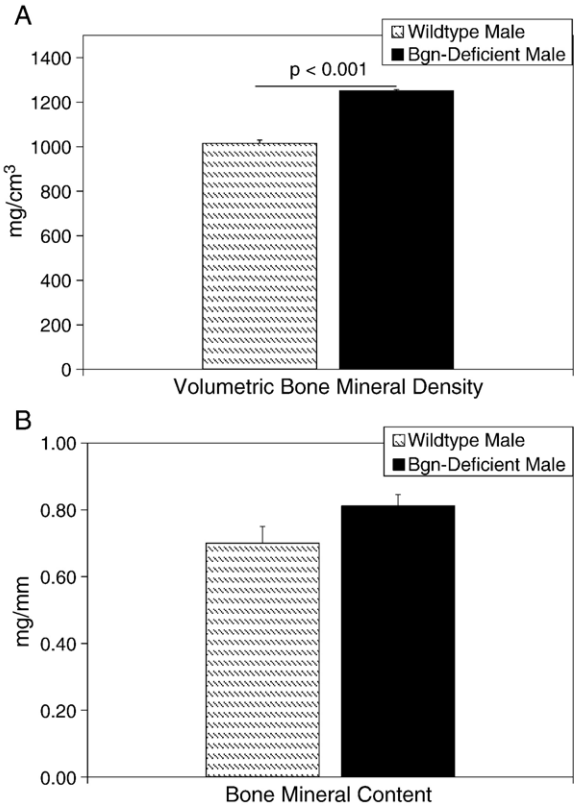

Fig. 4. Bone mineral quantification in the male tibial diaphysis of biglycan-deficient vs. wild type mice. 11-week-old bgn-deficient males had increased volumetric bone mineral density (A) in the tibial diaphyses compared with wild type males. Data are presented as mean ± SEM.

sites (femoral or tibial metaphyses or lumbar vertebrae) and/or a single cortical site. When characterizing the cortical bone phenotype of animals with an engineered genetic deficiency, the femoral diaphysis is the usual site chosen [11,17,20,39,45]. Data from this study demonstrate that, in some genetically compromised mice, the tibia exhibits a more pronounced phenotype, and evaluation of just the femora may be insufficient to characterize the phenotype.

The bgn-deficient male tibial diaphyses exhibited enhanced cross-sectional geometric properties compared with wild type males, including ML width and moment of inertia (Fig. 1). The contribution of material quantity to strength increases as the square of the distance from the centroid, and therefore a high moment of inertia is favorable for structural stiffness and strength. The AP/ML ratio, a measure of the structural anisotropy of the bone, was reduced to a value closer to 1 in the bgn-deficient males, indicating tissue which is more isotropically distributed around the bone's centroidal axis. An AP/ML ratio closer to 1 reiterates the increase in ML width and suggests a bone that is more resistant to bending in the ML direction, the direction of mechanical testing in this study. Looking at the geometric data alone, one would therefore predict that the bones of the bgn-deficient male mice would be structurally stronger. In the tibiae of the bgn-deficient male mice, this is not the case (Fig. 2D), indicating that geometric factors do not predict structural mechanical integrity.

Mineral is known to confer tissue-level stiffness and strength to bone. However, even though the volumetric bone mineral density (vBMD) was significantly increased in the cortical bone of the bgn-deficient male tibiae, there was a significant decrease in tissue-level yield strength. In this case, the result of a greater quantity of more highly mineralized tissue is a bone with lower structural pre-yield deformation and energy dissipation (Fig. 2). No correlations were noted between vBMD and any geometric or mechanical properties (data not shown). Energy dissipation negatively correlated with ML width (Fig. 5C, $r = -0.892$, $P < 0.001$) and moment of inertia (Fig. 5F, $r = -0.851$, $P < 0.001$). Similar correlations were found between ML width and moment of inertia and tissue-level strength and elastic deformation (Fig. 5). These pre-yield mechanical deficits reinforce the notion that mechanical properties are dependent on both tissue quantity and quality and increased quantity of material with an increased percentage of mineral may still be insufficient to increase structural mechanical properties if the quality of the tissue is poor.

The most likely interpretation for altered pre-yield properties is that the bgn gene deletion causes important alterations in mineral and/or the matrix/mineral ultrastructure. Bgn is most often implicated in the regulation of collagen fibril formation, size and morphology [26,32]. The organic matrix of bone, which is predominantly Type I collagen, dictates post-yield behavior in bone [3,9,52–56], so it is reasonable to hypothesize that if collagen were being affected in bgn-deficient mice, post-yield mechanical changes would be present. However, pre-yield properties were exclusively altered in this case, and this is likely the result of changes in the mineral compartment of bone versus matrix changes [3,57–59], suggesting a new understanding of the functional role of bgn in regulating bone mineralization in vivo. While SLRPs have not been directly implicated in the mineralization of bone in vivo, bgn has a strong affinity for apatite and calcium and facilitates initiation of apatite formation in vitro [33]. The ability for bgn to influence the mineral in bone in vivo is supported by the increase in volumetric bone mineral density in the bgn-deficient male tibial diaphysis (Fig. 4) and locally altered mineral content and mineral to matrix ratios [24]. As bone in bgn-deficient mice is developing, the altered quality of the tissue may activate a compensatory increase in matrix formation and/or mineralization in an attempt to redistribute the tissue to a more structurally isotropic configuration with greater moment of inertia. It is also possible that the lack of bgn is influencing the integrity of the collagen network, and because the organic matrix forms the scaffold for mineral formation, changes in collagen could induce detrimental alterations in mineral organization leading to the decrease in strength noted [9,52,60].

It might seem contradictory that there were no differences in histomorphometric measures in the bgn-deficient male tibial diaphyses versus wild type animals, though large differences were noted in geometric properties. What we can conclude is that, during the window of time observed with fluorochrome labels, BFR was not greater in the bgn-deficient males. However, injections were given at Day −20 and −6 and therefore only measured BFR during weeks 8 and 10 of life.

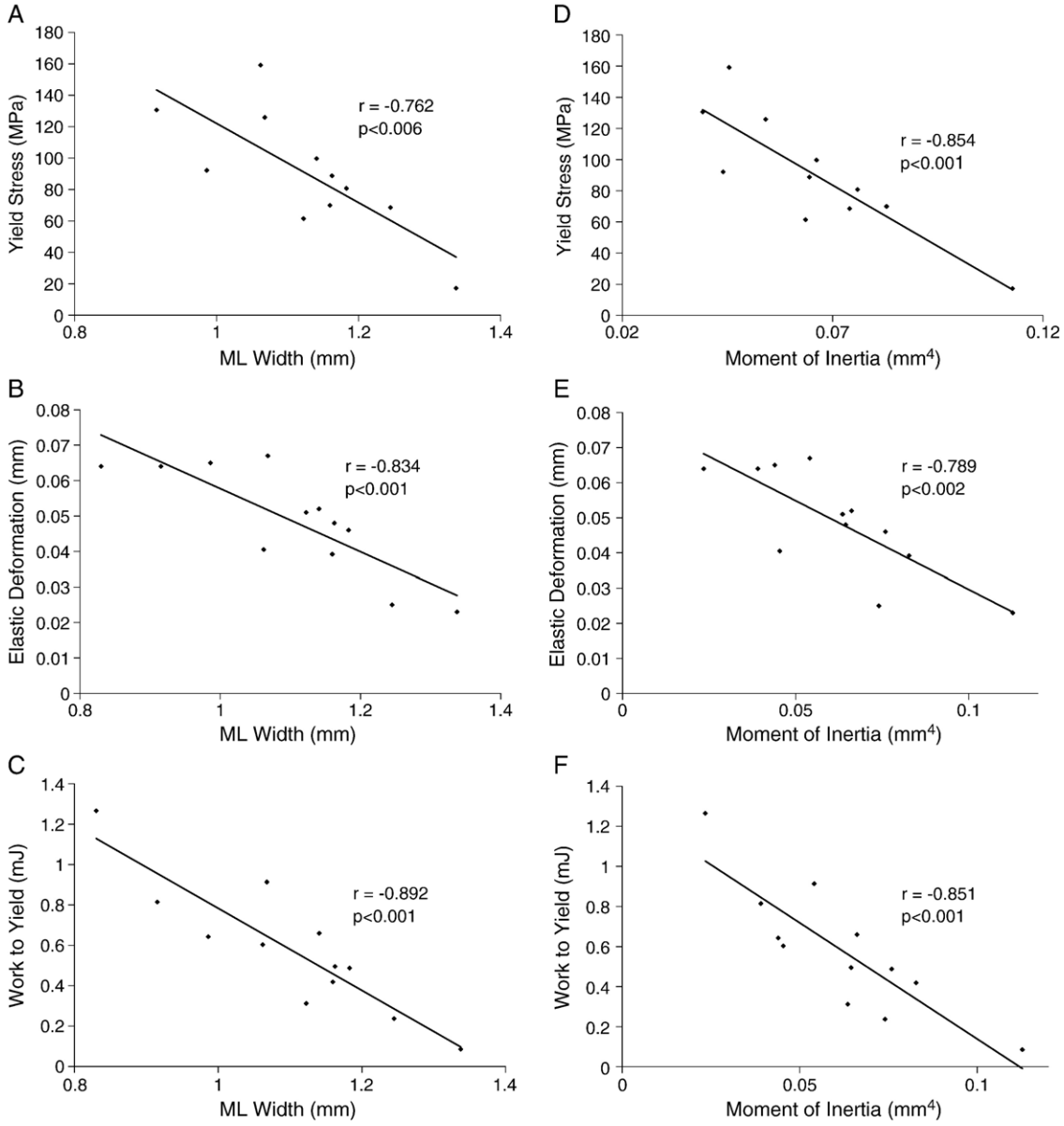

Fig. 5. Correlations of structural and tissue-level mechanical properties to geometric properties of the biglycan-deficient male tibial diaphyses. ML width and moment of inertia in the bgn-deficient males are negatively correlated with tissue-level yield strength (A and D). Structural elastic deformation (B and E) and structural work-to-yield (C and F).

Therefore, the bone formation that led to greater geometric properties in the bgn-deficient mice likely occurred before this age and had slowed down by the time it was measured. This is consistent with the idea that osteopenia and decreased osteoblast activity caused by biglycan deficiency are age-dependent and become progressively worse as the animal ages [39].

The significant difference in body weight between bgn-deficient and wild type males is likely not responsible for the differences in tibial properties between genotypes. If body weight were having an effect, the lower body weight in the bgn-deficient males would impart lesser loads on the tibia, producing lower strains and a lesser bone formation response. Male tibial properties were normalized by body weight (data not shown), and, while significance was marginalized in some cases (yield stress, work-to-yield) or disappeared (elastic deformation, length), other properties showed increased significance (ML width, moment of inertia) or newly acquired significance (increased cortical area, increased AP width, increased cortical thickness), and all trends were still in the same direction. Furthermore, similar differences in body weight exist in bgn-deficient females versus wild type females, with no corresponding alteration in tibial properties. This suggests that, while the body weight difference may play a role, it is alone not responsible for the altered properties of the bgn-deficient male tibiae.

There are some factors which may help explain the bone specificity seen in the male mice in response to bgn deficiency. Studies between inbred mouse strains have demonstrated that bone mechanical properties [14–17] as well as the mechanical

Table 3
Tissue-level mechanical properties of the male and female femoral diaphyses of biglycan-deficient vs. wild type mice

Group	Yield stress (MPa)	Ultimate stress (MPa)	Strain to failure (με)	Modulus of elasticity (GPa)
Male femora (wild type)	**62.75 ± 10.10**	85.05 ± 11.64	36,000 ± 5446	3.13 ± 0.50
Male femora (bgn-deficient)	**43.69 ± 2.52**[a]	74.69 ± 5.24	31,625 ± 2097	3.20 ± 0.21
Female femora (wild type)	73.47 ± 4.03	101.49 ± 3.00	31,804 ± 4617	5.26 ± 0.19
Female femora (bgn-deficient)	68.02 ± 8.06	85.35 ± 10.28	21,625 ± 2135	5.96 ± 1.99

Data are presented as mean ± SEM. [a]Indicates $P < 0.05$ vs. wild type for the same gender. Significant differences are bolded for ease of interpretation.

response of bones to the local environment [21,22,61,62] are under genetic control. It is possible that the specific genetic deficiency in this study impacts osteoblast progenitors, and therefore bone properties, in certain bones and not in others, leading to the bone specificity demonstrated. The mapping of quantitative trait loci (QTLs) [11,13,42,43] for individual bone traits is a powerful tool and is rapidly uncovering discrete chromosomal locations that affect geometric parameters in individual bones. A second, but less likely factor is related to the observation that collagen fibrils in tendons from bgn-deficient mice are structurally and mechanically altered, resulting in joint laxity, gait impairment and early-onset osteoarthritis [32]. If differences were present in the joints of bgn-deficient mice, this may cause the femora and tibiae to be exposed to different loading states during normal activity than the same bones from wild type animals, possibly influencing the dimorphism in phenotype noted between these two bones. However, bgn-deficient mice demonstrated no gait impairment up to 11 weeks of age and were able to run on a treadmill with no noticeable problems and no differences in gait compared with wild type animals [63], suggesting that the problem of joint laxity was not present in this study.

The mechanical phenotype in females was more subtle than in males and was almost completely femoral-specific. Bgn deficiency has minimal effects on basal bone metabolism in the proximal tibiae of 6-month-old female mice [40], but the femora were not examined and no geometric or mechanical indices were measured in this study. The mechanisms behind the gender specificity seen in the current study are unknown. Estrogen-receptor-β-deficient [44] and aromatase-deficient [45] mice both showed gender differences in bone properties, but these two molecules are responsible for interactions with estrogen so sexual dimorphism can be expected. It is possible that the gender-specific response in bgn-deficient mice is connected to estrogen, and this is supported by work showing that bgn-deficient females are protected from the trabecular bone loss normally associated with ovariectomy [40].

While hormones likely contribute to the sexual dimorphism observed in this study, other possible explanations exist. Congenic mouse studies and QTL analyses reveal sex-specific regulation of certain skeletal characteristics [11–13]. Furthermore, because the gene encoding bgn lies on the X chromosome, the genetic insult in this study may have affected the genes responsible for regulating some bone properties in males while bypassing the genes in females. Whatever the cause, female mice are spared most of the deleterious effects in cortical bone caused by this genetic insult.

Some of the data presented here differ from previously published work on bgn-deficient mice. The enhancement in geometric properties in 11-week-old bgn-deficient males versus wild type males (Fig. 1) is in contrast to a decrease in average cortical thickness noted in the femoral diaphysis [39], though these data were from 9-month-old-mice. This previous study showed no femoral changes, consistent with our data at 11 weeks. At 11 weeks, mice are still in a state of growth, while at 9 months, the mice have finished growth. Trends toward increased tibial endocortical histomorphometric indices seen in the current study contrast with decreases in the same indices in the femoral metaphyses of 3-month-old-mice [39], reinforcing the site-specific effects of genetic alterations.

There are several methodological considerations worthy of discussion. pQCT was performed only on male bones for two reasons. First, the geometric and mechanical phenotypes were displayed in males, indicating that the females may be protected from the deleterious effects of the gene deletion in cortical bone. Second, bone mineral density in the proximal tibiae of bgn-deficient females was unchanged from wild type female levels at 6 months, while bgn-deficient male tibiae showed a significant decrease in vBMD compared to wild type males [40]. Since the bgn-deficient phenotype is known to be age-dependent [39], and no bone mineral phenotype was seen in the females at 6 months, it is unlikely that there would be a mineral-related phenotype in female bones at 11 weeks.

It is important to point out that limitations do exist when making area and density measurements of mouse bones using pQCT [64,65]. These values depend on specimen thickness, as one would expect when trying to clearly define the edges of a bone that has a cortical thickness of ~200 μm using a resolution of 70 μm. A key point is that much of this error occurs when trying to make comparisons among groups differing in cortical thickness. Since the mean cortical thickness of each group in this study was not statistically different, any partial volume effects pertinent to vBMD and BMC measures should be consistent among groups.

In summary, the mechanical phenotype associated with targeted disruption of biglycan is both bone- and gender-specific in mice at 11 weeks of age. The bgn-deficient male tibiae exhibited improved cross-sectional geometric properties and greater bone mineral density compared to their wild type counterparts, while having lower tissue-level yield strength and structural pre-yield deformation and energy dissipation. Because pre-yield properties alone were impacted, this implies that the gene deletion causes important alterations in mineral and/or the matrix/mineral ultrastructure, suggesting a new

understanding of the functional role of bgn in regulating bone mineralization in vivo.

Acknowledgments

DoD Army DAMD17-03-1-0556; NIH T32-DE07057; NIH IPA agreement; Regenerative Sciences Training Grant R90-DK071506; Tina Kilts for help genotyping mice.

References

[1] Baron R. General principles of bone biology. Primer on the metabolic bone diseases and disorders of mineral metabolism. The American Society for Bone and Mineral Research; 2004. p. 1–8.
[2] Burr DB, Turner CH. Biomechanics of bone. Primer on the metabolic bone diseases and disorders of mineral metabolism. The American Society for Bone and Mineral Research; 2004. p. 58–64.
[3] Burstein AH, Zika JM, Heiple KG, Klein L. Contribution of collagen and mineral to the elastic-plastic properties of bone. J Bone Joint Surg Am 1975;57:956–61.
[4] Currey JD. The effect of porosity and mineral content on the Young's modulus of elasticity of compact bone. J Biomech 1988;21:131–9.
[5] Martin RB, Ishida J. The relative effects of collagen fiber orientation, porosity, density, and mineralization on bone strength. J Biomech 1989;22:419–26.
[6] Martin RB, Boardman DL. The effects of collagen fiber orientation, porosity, density, and mineralization on bovine cortical bone bending properties. J Biomech 1993;26:1047–54.
[7] Landis WJ. The strength of a calcified tissue depends in part on the molecular structure and organization of its constituent mineral crystals in their organic matrix. Bone 1995;16:533–44.
[8] Ferguson VL, Ayers RA, Bateman TA, Simske SJ. Bone development and age-related bone loss in male C57BL/6J mice. Bone 2003;33:387–98.
[9] Wang X, Shen X, Li X, Agrawal CM. Age-related changes in the collagen network and toughness of bone. Bone 2002;31:1–7.
[10] Duan Y, Beck TJ, Wang XF, Seeman E. Structural and biomechanical basis of sexual dimorphism in femoral neck fragility has its origins in growth and aging. J Bone Miner Res 2003;18:1766–74.
[11] Turner CH, Sun Q, Schriefer J, Pitner N, Price R, Bouxsein ML, et al. Congenic mice reveal sex-specific genetic regulation of femoral structure and strength. Calcif Tissue Int 2003;73:297–303.
[12] Klein RF, Turner RJ, Skinner LD, Vartanian KA, Serang M, Carlos AS, et al. Mapping quantitative trait loci that influence femoral cross-sectional area in mice. J Bone Miner Res 2002;17:1752–60.
[13] Orwoll ES, Belknap JK, Klein RF. Gender specificity in the genetic determinants of peak bone mass. J Bone Miner Res 2001;16:1962–71.
[14] Akhter MP, Iwaniec UT, Covey MA, Cullen DM, Kimmel DB, Recker RR. Genetic variations in bone density, histomorphometry, and strength in mice. Calcif Tissue Int 2000;67:337–44.
[15] Jepsen KJ, Pennington DE, Lee YL, Warman M, Nadeau J. Bone brittleness varies with genetic background in A/J and C57BL/6J inbred mice. J Bone Miner Res 2001;16:1854–62.
[16] Sheng MH, Baylink DJ, Beamer WG, Donahue LR, Lau KH, Wergedal JE. Regulation of bone volume is different in the metaphyses of the femur and vertebra of C3H/HeJ and C57BL/6J mice. Bone 2002;30:486–91.
[17] Turner CH, Hsieh YF, Muller R, Bouxsein ML, Baylink DJ, Rosen CJ, et al. Genetic regulation of cortical and trabecular bone strength and microstructure in inbred strains of mice. J Bone Miner Res 2000;15:1126–1131.
[18] Iwamoto J, Yeh JK, Aloia JF. Differential effect of treadmill exercise on three cancellous bone sites in the young growing rat. Bone 1999;24:163–9.
[19] Mosekilde L, Thomsen JS, Orhii PB, McCarter RJ, Mejia W, Kalu DN. Additive effect of voluntary exercise and growth hormone treatment on bone strength assessed at four different skeletal sites in an aged rat model. Bone 1999;24:71–80.
[20] Turner CH, Hsieh YF, Muller R, Bouxsein ML, Rosen CJ, McCrann ME, et al. Variation in bone biomechanical properties, microstructure, and density in BXH recombinant inbred mice. J Bone Miner Res 2001;16:206–13.
[21] Robling AG, Turner CH. Mechanotransduction in bone: genetic effects on mechanosensitivity in mice. Bone 2002;31:562–9.
[22] Kodama Y, Umemura Y, Nagasawa S, Beamer WG, Donahue LR, Rosen CR, et al. Exercise and mechanical loading increase periosteal bone formation and whole bone strength in C57BL/6J mice but not in C3H/Hej mice. Calcif Tissue Int 2000;66:298–306.
[23] Carter DR, Van Der Meulen MC, Beaupre GS. Mechanical factors in bone growth and development. Bone 1996;18:5S–10S.
[24] Corsi A, Xu T, Chen XD, Boyde A, Liang J, Mankani M, et al. Phenotypic effects of biglycan deficiency are linked to collagen fibril abnormalities, are synergized by decorin deficiency, and mimic Ehlers–Danlos-like changes in bone and other connective tissues. J Bone Miner Res 2002;17:1180–9.
[25] Wiberg C, Hedbom E, Khairullina A, Lamande SR, Oldberg A, Timpl R, et al. Biglycan and decorin bind close to the n-terminal region of the collagen VI triple helix. J Biol Chem 2001;276:18947–52.
[26] Schonherr E, Witsch-Prehm P, Harrach B, Robenek H, Rauterberg J, Kresse H. Interaction of biglycan with type I collagen. J Biol Chem 1995;270:2776–83.
[27] Hocking AM, Shinomura T, McQuillan DJ. Leucine-rich repeat glycoproteins of the extracellular matrix. Matrix Biol 1998;17:1–19.
[28] Chen XD, Fisher LW, Robey PG, Young MF. The small leucine-rich proteoglycan biglycan modulates BMP-4-induced osteoblast differentiation. FASEB J 2004;18:948–58.
[29] Ruoslahti E. Proteoglycans in cell regulation. J Biol Chem 1989;264:13369–13372.
[30] Takagi M, Yamada T, Kamiya N, Kumagai T, Yamaguchi A. Effects of bone morphogenetic protein-2 and transforming growth factor-beta1 on gene expression of decorin and biglycan by cultured osteoblastic cells. Histochem J 1999;31:403–9.
[31] Yamada T, Kamiya N, Harada D, Takagi M. Effects of transforming growth factor-beta1 on the gene expression of decorin, biglycan, and alkaline phosphatase in osteoblast precursor cells and more differentiated osteoblast cells. Histochem J 1999;31:687–94.
[32] Ameye L, Young MF. Mice deficient in small leucine-rich proteoglycans: novel in vivo models for osteoporosis, osteoarthritis, Ehlers–Danlos syndrome, muscular dystrophy, and corneal diseases. Glycobiology 2002;12:107R–16R.
[33] Boskey AL, Spevak L, Doty SB, Rosenberg L. Effects of bone CS-proteoglycans, DS-decorin, and DS-biglycan on hydroxyapatite formation in a gelatin gel. Calcif Tissue Int 1997;61:298–305.
[34] Bianco P, Fisher LW, Young MF, Termine JD, Robey PG. Expression and localization of the two small proteoglycans biglycan and decorin in developing human skeletal and non-skeletal tissues. J Histochem Cytochem 1990;38:1549–63.
[35] Fisher LW, Termine JD, Dejter Jr SW, Whitson SW, Yanagishita M, Kimura JH, et al. Proteoglycans of developing bone. J Biol Chem 1983;258:6588–94.
[36] Fisher LW, Termine JD, Young MF. Deduced protein sequence of bone small proteoglycan I (biglycan) shows homology with proteoglycan II (decorin) and several nonconnective tissue proteins in a variety of species. J Biol Chem 1989;264:4571–6.
[37] Chen XD, Allen MR, Bloomfield S, Xu T, Young M. Biglycan-deficient mice have delayed osteogenesis after marrow ablation. Calcif Tissue Int 2003;72:577–82.
[38] Chen XD, Shi S, Xu T, Robey PG, Young MF. Age-related osteoporosis in biglycan-deficient mice is related to defects in bone marrow stromal cells. J Bone Miner Res 2002;17:331–40.
[39] Xu T, Bianco P, Fisher LW, Longenecker G, Smith E, Goldstein S, et al. Targeted disruption of the biglycan gene leads to an osteoporosis-like phenotype in mice. Nat Genet 1998;20:78–82.
[40] Nielsen KL, Allen MR, Bloomfield SA, Andersen TL, Chen XD, Poulsen HS, et al. Biglycan deficiency interferes with ovariectomy-induced bone loss. J Bone Miner Res 2003;18:2152–8.
[41] Yershov Y, Baldini TH, Villagomez S, Young T, Martin ML, Bockman RS,

et al. Bone strength and related traits in HcB/Dem recombinant congenic mice. J Bone Miner Res 2001;16:992–1003.
[42] Shultz KL, Donahue LR, Bouxsein ML, Baylink DJ, Rosen CJ, Beamer WG. Congenic strains of mice for verification and genetic decomposition of quantitative trait loci for femoral bone mineral density. J Bone Miner Res 2003;18:175–85.
[43] Volkman SK, Galecki AT, Burke DT, Paczas MR, Moalli MR, Miller RA, et al. Quantitative trait loci for femoral size and shape in a genetically heterogeneous mouse population. J Bone Miner Res 2003;18:1497–505.
[44] Sims NA, Dupont S, Krust A, Clement-Lacroix P, Minet D, Resche-Rigon M, et al. Deletion of estrogen receptors reveals a regulatory role for estrogen receptors-beta in bone remodeling in females but not in males. Bone 2002;30:18–25.
[45] Oz OK, Zerwekh JE, Fisher C, Graves K, Nanu L, Millsaps R, et al. Bone has a sexually dimorphic response to aromatase deficiency. J Bone Miner Res 2000;15:507–14.
[46] Moore DS, McCabe GP. Introduction to the practice of statistics. 4th ed. New York, NY: W.H. Freeman and Company; 2003.
[47] Gustafson MB, Martin RB, Gibson V, Storms DH, Stover SM, Gibeling J, et al. Calcium buffering is required to maintain bone stiffness in saline solution. J Biomech 1996;29:1191–4.
[48] Rajachar R.M. Effects of age-related ultra-structural changes in bone on microdamage mechanisms. PhD Dissertation. The University of Michigan; 2003.
[49] H.J. Sommer, Polygeom Matlab Function. Available at http://www.me.psu.edu/sommer/me562/polygeom.m. Accessed July 1, 2002.
[50] Parfitt AM, Drezner MK, Glorieux FH, Kanis JA, Malluche H, Meunier PJ, et al. Bone histomorphometry: standardization of nomenclature, symbols, and units. Report of the ASBMR Histomorphometry Nomenclature Committee. J Bone Miner Res 1987;2:595–610.
[51] Sakakura Y, Shide N, Tsuruga E, Irie K, Yajima T. Effects of running exercise on the mandible and tibia of ovariectomized rats. J Bone Miner Metab 2001;19:159–67.
[52] Boskey AL, Wright TM, Blank RD. Collagen and bone strength. J Bone Miner Res 1999;14:330–5.
[53] Burr DB. The contribution of the organic matrix to bone's material properties. Bone 2002;31:8–11.
[54] Currey JD, Foreman J, Laketic I, Mitchell J, Pegg DE, Reilly GC. Effects of ionizing radiation on the mechanical properties of human bone. J Orthop Res 1997;15:111–7.
[55] Wang X, Bank RA, TeKoppele JM, Agrawal CM. The role of collagen in determining bone mechanical properties. J Orthop Res 2001;19:1021–6.
[56] Wang X, Li X, Bank RA, Agrawal CM. Effects of collagen unwinding and cleavage on the mechanical integrity of the collagen network in bone. Calcif Tissue Int 2002;71:186–92.
[57] Alho A, Husby T, Hoiseth A. Bone mineral content and mechanical strength. An ex vivo study on human femora at autopsy. Clin Orthop Relat Res 1988;227:292–7.
[58] Follet H, Boivin G, Rumelhart C, Meunier PJ. The degree of mineralization is a determinant of bone strength: a study on human calcanei. Bone 2004;34:783–9.
[59] Wachter NJ, Krischak GD, Mentzel M, Sarkar MR, Ebinger T, Kinzl L, et al. Correlation of bone mineral density with strength and microstructural parameters of cortical bone in vitro. Bone 2002;31:90–5.
[60] Oxlund H, Barckman M, Ortoft G, Andreassen TT. Reduced concentrations of collagen cross-links are associated with reduced strength of bone. Bone 1995;17:365S–71S.
[61] Akhter MP, Cullen DM, Pedersen EA, Kimmel DB, Recker RR. Bone response to in vivo mechanical loading in two breeds of mice. Calcif Tissue Int 1998;63:442–9.
[62] Kodama Y, Dimai HP, Wergedal J, Sheng M, Malpe R, Kutilek S, et al. Cortical tibial bone volume in two strains of mice: effects of sciatic neurectomy and genetic regulation of bone response to mechanical loading. Bone 1999;25:183–90.
[63] Wallace JM, Rajachar RM, Chen X, Shi S, Allen MR, Bloomfield SA, et al. The phenotype of biglycan-deficient mice can be modified by mechanical loading, paper no. 197, 2004 Annual Meeting of the Orthopaedic Society.
[64] Brodt MD, Pelz GB, Taniguchi J, Silva MJ. Accuracy of peripheral quantitative computed tomography (pQCT) for assessing area and density of mouse cortical bone. Calcif Tissue Int 2003;73:411–8.
[65] Schmidt C, Priemel M, Kohler T, Weusten A, Muller R, Amling M, et al. Precision and accuracy of peripheral quantitative computed tomography (pQCT) in the mouse skeleton compared with histology and microcomputed tomography (microCT). J Bone Miner Res 2003;18:1486–96.